

Supporting Information

Solvatomorphism, polymorphism and spin crossover in bis[hydrotris(1,2,3-triazol-1-yl)borate]iron(II)

Oleksandr Ye. Horniichuk,^{ab} Karl Ridier,^b Gábor Molnár,^b Volodymyr O. Kotsyubynsky,^d Sergiu Shova,^c Vladimir M. Amirkhanov,^a Il'ya A. Gural'skiy,^{*a} Lionel Salmon,^{*b} Azzedine Bousseksou^b

^a Taras Shevchenko National University of Kyiv, Faculty of Chemistry, 12, Lva Tolstogo str., 01033, Kyiv, Ukraine

^b LCC, CNRS and Université de Toulouse (UPS, INP) 205 route de Narbonne, F-31077 Toulouse, France

^c "Petru Poni" Institute of Macromolecular Chemistry, 41A Aleea Gr. Ghica Voda, 700487 Iasi, Romania

^d Department of Material Science and New Technology, Vasyl Stefanyk Precarpathian National University, Ivano-Frankivsk 76018, Ukraine

I- Structural data

II- Raman Spectroscopy

III- Mössbauer spectroscopy

IV- References

I- Structural data

Table S1. Crystal data and structure refinement of solvatomorphs.

Compound	1·2DMSO	1·7DMSO	1·2MeOH	1·2CHCl ₃	1·2DMF·H ₂ O	1
Formula weight	644.14	1034.74	551.96	726.62	652.09	487.88
Temperature (K)	293	160	180	180	293	293
Space group	<i>P</i> 1	<i>R</i> ³ _c	<i>P</i> 2 ₁ / <i>n</i>	<i>P</i> 2 ₁ / <i>c</i>	<i>P</i> bcn	<i>P</i> 2 ₁ / <i>c</i>
<i>a</i> (Å)	8.3929(13)	13.3415(3)	10.4567(8)	8.2460(4)	8.3469(5)	8.2563(13)
<i>b</i> (Å)	9.0045(15)	13.3415(3)	8.2415(5)	12.1991(4)	15.7421(7)	8.2491(19)
<i>c</i> (Å)	10.0309(16)	48.9618(11)	13.9101(8)	14.6014(6)	22.5116(9)	15.902(4)
α , (°)	86.465(13)	90	90	90	90	90
β , (°)	84.490(13)	90	99.208(7)	105.973(4)	90	100.91(2)
γ , (°)	65.635(16)	120	90	90	90	90
Cell volume, (Å ³)	687.2(2)	7547.4(4)	1183.31(14)	1412.11(10)	2958.0(3)	1063.5(4)
<i>Z</i>	1	6	2	2	4	2
ρ_{calc} (g/cm ³)	1.557	1.358	1.549	1.709	1.464	1.524
μ (mm ⁻¹)	0.755	0.647	0.692	1.147	0.570	0.753
Reflections collected/unique	5142/2408	10071/2021	8240/2322	9532/3251	10062/2601	2425/2425
GoF	0.996	1.060	1.084	1.047	1.053	1.104
Final <i>R</i> indices [<i>I</i> >2σ(<i>I</i>)]	<i>R</i> ₁ =0.0591, <i>wR</i> ₂ =0.0894	<i>R</i> ₁ =0.0441, <i>wR</i> ₂ =0.1023	<i>R</i> ₁ =0.0538, <i>wR</i> ₂ =0.0862	<i>R</i> ₁ =0.0403, <i>wR</i> ₂ =0.0802	<i>R</i> ₁ =0.0537, <i>wR</i> ₂ =0.0945	<i>R</i> ₁ =0.2410, <i>wR</i> ₂ =0.5271
R indices (all data)	<i>R</i> ₁ =0.0944, <i>wR</i> ₂ =0.1033	<i>R</i> ₁ =0.0577, <i>wR</i> ₂ =0.1088	<i>R</i> ₁ =0.0768, <i>wR</i> ₂ =0.0932	<i>R</i> ₁ =0.0519, <i>wR</i> ₂ =0.0848	<i>R</i> ₁ =0.0890, <i>wR</i> ₂ =0.1082	<i>R</i> ₁ =0.2663, <i>wR</i> ₂ =0.5393
CCDC	2161995	2161996	2161997	2161994	2161998	2161993

Table S2. Selected bond distances and angles of the solvatomorphs

Compound	1·2DMSO	1·7DMSO	1·2MeOH	1·2CHCl ₃	1·2DMF·H ₂ O	1
Distance, Å						
Fe–N(1)	1.959(3)	1.9674(18)	1.955(2)	1.9600(19)	1.968(3)	1.991(14)
Fe–N(2)	1.959(3)	1.9676(17)	1.955(2)	1.9600(19)	1.968(3)	1.991(14)
Fe–N(3)	1.952(3)	1.9676(17)	1.958(2)	1.9468(18)	1.958(3)	1.931(18)
Fe–N(4)	1.952(3)	1.9676(18)	1.958(2)	1.9468(18)	1.958(3)	1.931(19)
Fe–N(5)	1.964(3)	1.9676(17)	1.972(2)	1.9597(18)	1.964(2)	1.950(15)
Fe–N(6)	1.964(3)	1.9676(17)	1.972(2)	1.9597(18)	1.964(2)	1.950(15)
Angle, ° (average value)						
Cis (intra)	88.27(13)	87.91(7)	88.11(10)	88.55(8)	88.16(11)	88.07(7)
Cis (inter)	91.73(13)	92.09(7)	91.89(10)	91.45(8)	91.84(11)	91.93(7)
Trans	180.0	180.00(9)	180.00(8)	180.00(3)	180.0	180.0

Table S3. Selected structural parameters comparison for tris(triazolyl)- and tris(pyrazolyl)borate ferrous complexes.

Compound	[Fe(HB(1,2,3-tz) ₃) ₂]	[Fe(HB(1,2,4-tz) ₃) ₂] ¹	[Fe(HB(pz) ₃) ₂] ²
Space group	<i>P</i> 2 ₁ / <i>c</i>	<i>P</i> bcn	<i>P</i> 2 ₁ / <i>c</i>
Distance, Å			
Fe–N(1)	1.991(14)	1.9822(11)	1.973(3)
Fe–N(2)	1.991(14)	1.9822(11)	1.980(3)
Fe–N(3)	1.931(18)	1.9754(11)	1.972(3)
Fe–N(4)	1.931(18)	1.9754(11)	1.979(3)
Fe–N(5)	1.950(15)	1.9758(11)	1.960(3)
Fe–N(6)	1.950(15)	1.9758(11)	1.971(4)
Fe···Fe (along <i>a</i> -axis)	8.2563(13)	7.97820(18)	8.4403(13)
Fe···Fe (along <i>b</i> -axis)	8.2491(19)	9.8678(2)	11.606(2)
Fe···Fe (along <i>c</i> -axis)	8.9571(18)	8.7654(2)	8.674(2)
Volume, Å ³			
Coordination octahedron	9.97	10.30	10.21
Unit cell volume per molecule	516.6	531.8	560.1

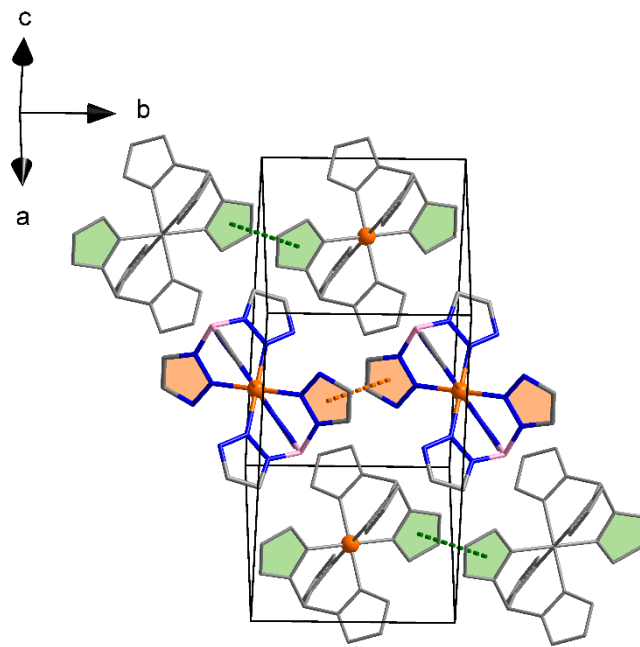


Figure S1. Unit cell of **1** with displayed π - π stacking interactions propagating along two opposite directions within *ab*-plane. Hydrogen atoms are omitted for clarity.

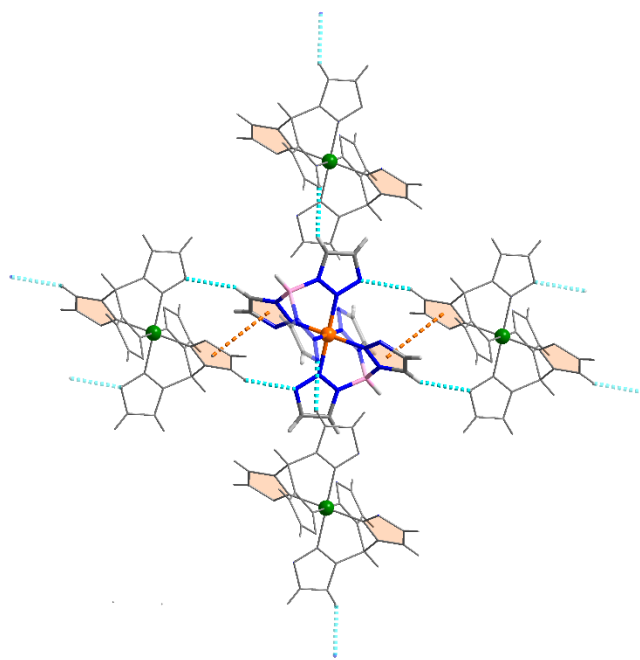


Figure S2. Crystal packing in **1** with intermolecular interactions (π - π stacking interactions are shown only for one direction).

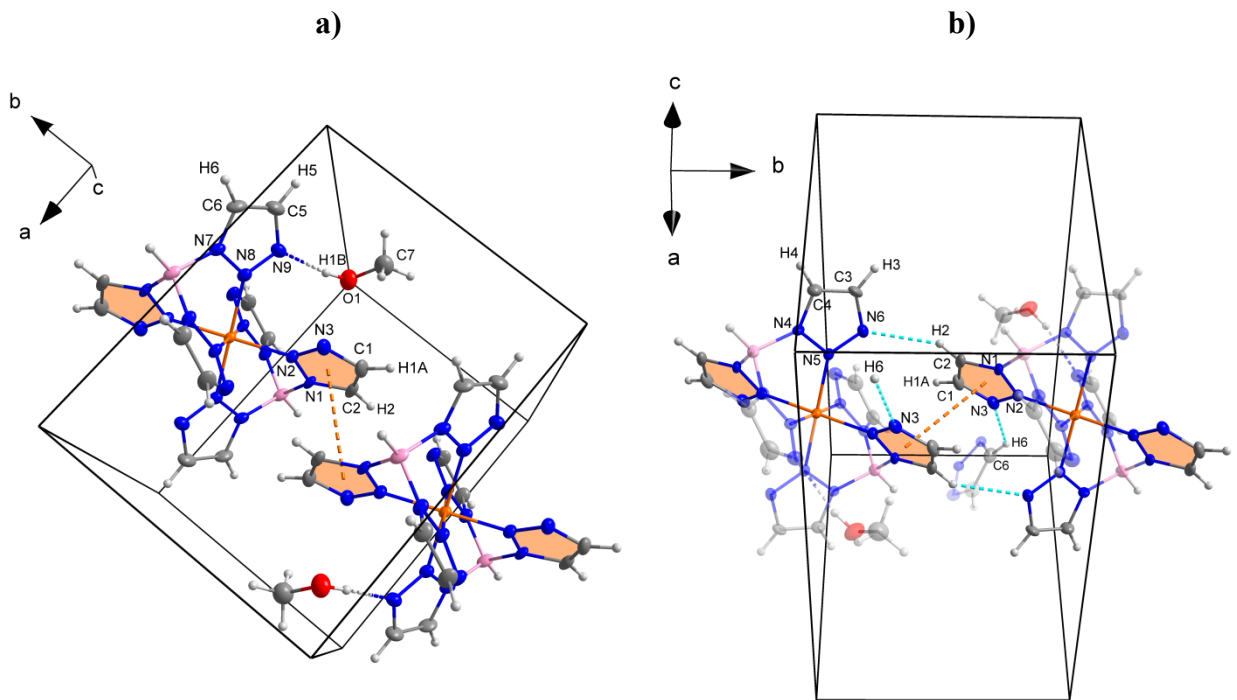


Figure S3. Fragments of **1·2MeOH** crystal structure, where hydrogen bonding between **FeL₂** and MeOH molecules (a), C–H···N interactions (b) and intermolecular π - π stacking (a, b) are shown. Parts of the molecules in b are omitted or made transparent for clarity.

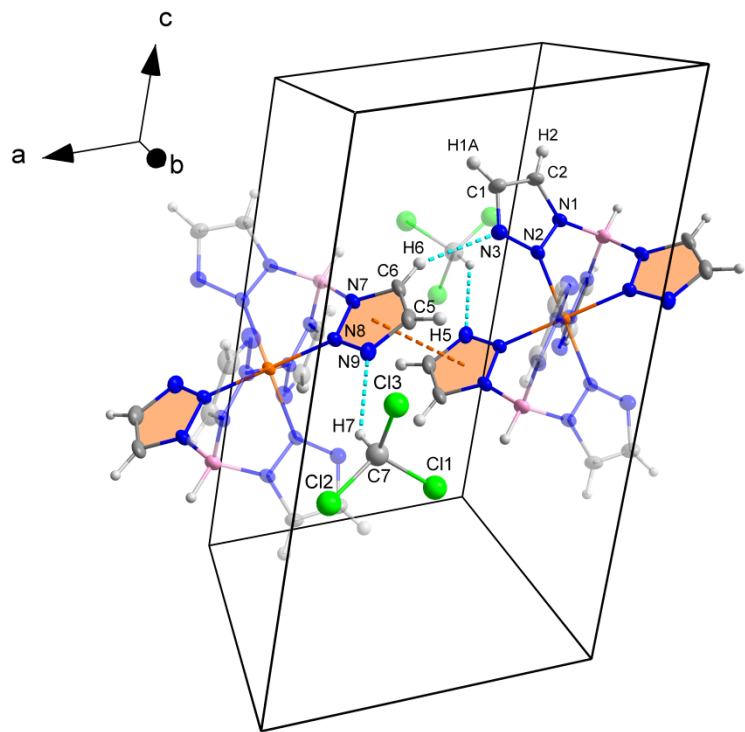


Figure S4. **1·2CHCl₃** crystal structure fragment with intermolecular interactions between the complex and the solvent molecules. Parts of **[Fe(HB(1,2,3-tz)₃)₂]** molecules are represented transparent for clarity.

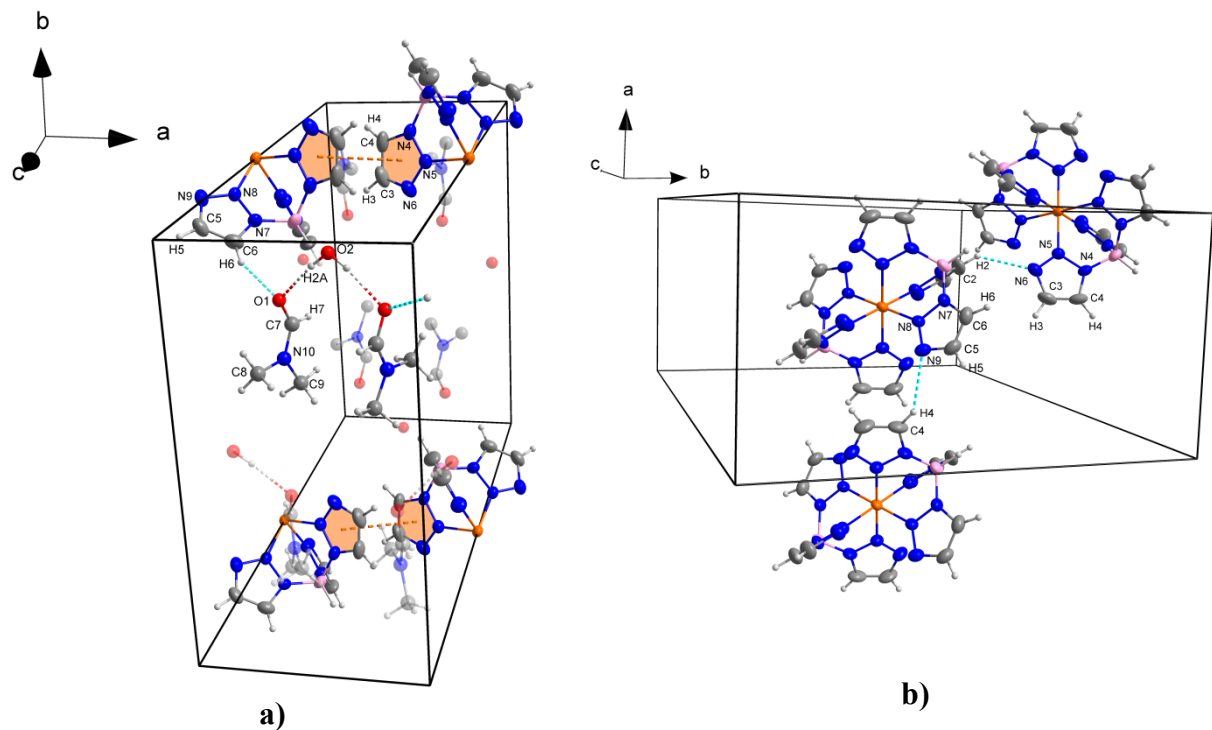


Figure S5. Fragments of **1·2DMF·H₂O** crystal structure representing intermolecular C–H···O contacts, π–π stacking (**a**) and C–H···N (**b**) interactions.

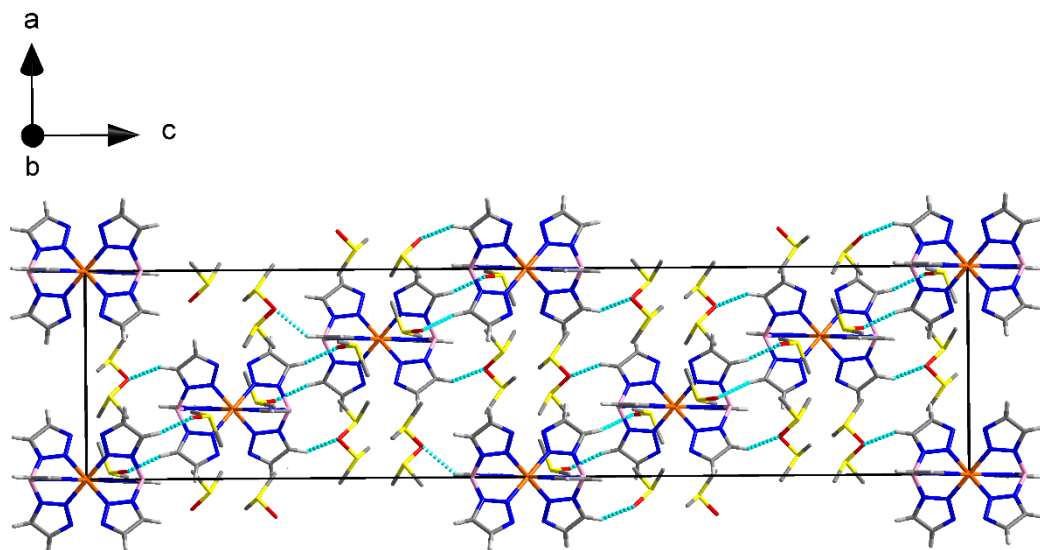


Figure S6. Crystal structure (packing diagram) of **1·7DMSO** solvatomorph with intermolecular interactions shown. Hydrogen atoms of the disordered CH₃-moieties of the solvent are omitted for clarity.

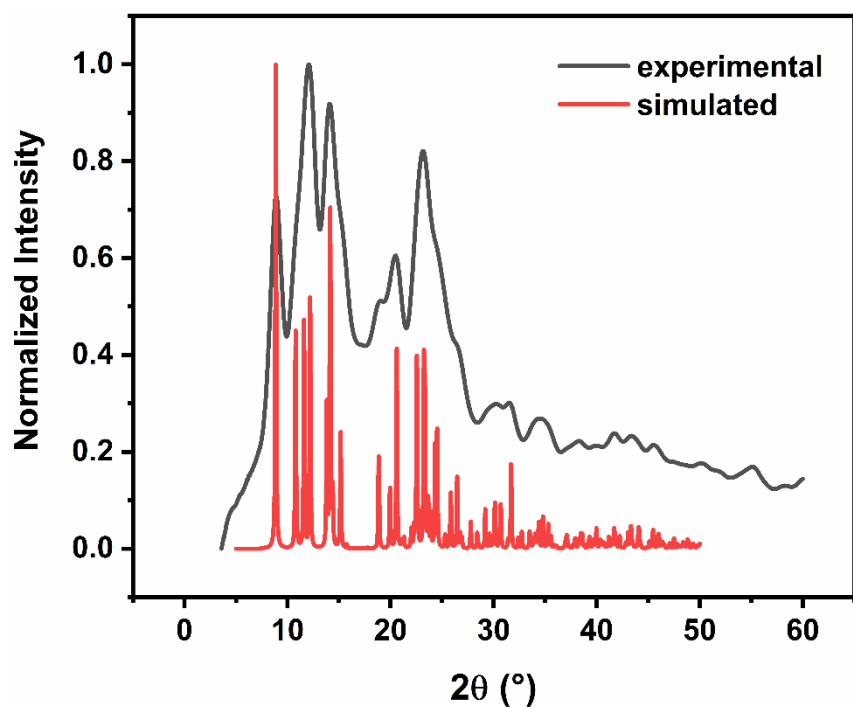


Figure S7. Simulated PXRD pattern of **1·2DMSO** versus experimental PXRD pattern recorded for desolvated **1·7DMSO** crystals.

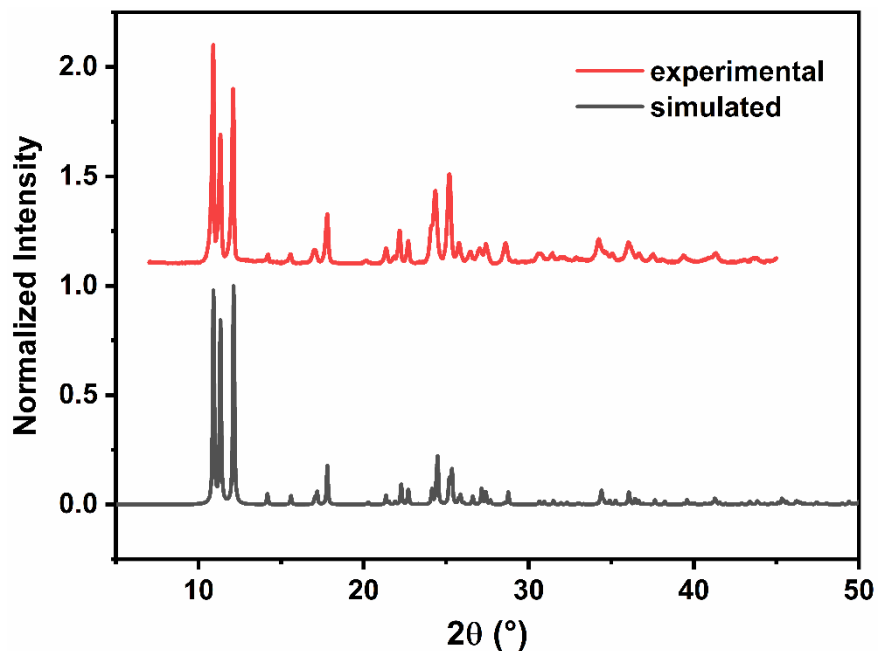


Figure S8. Experimental and simulated PXRD patterns of **1**.

II- Raman Spectroscopy

The Raman spectra were collected for dehydrated crystal of **1** in 303-433 K range (Fig. S9a). The spectra revealed reversibility upon cooling to room temperature at the end of the thermal cycle. Intensity of the signals in 1160-1280 cm⁻¹ region of the spectra tends to decrease upon heating, that makes them useful to track the spin crossover properties. Plotting integral intensity ratio of the bands at 1205 cm⁻¹ and 1263 cm⁻¹ versus temperature yields the spin crossover curve, that is in accordance with magnetic measurements' data (Figure S9b).

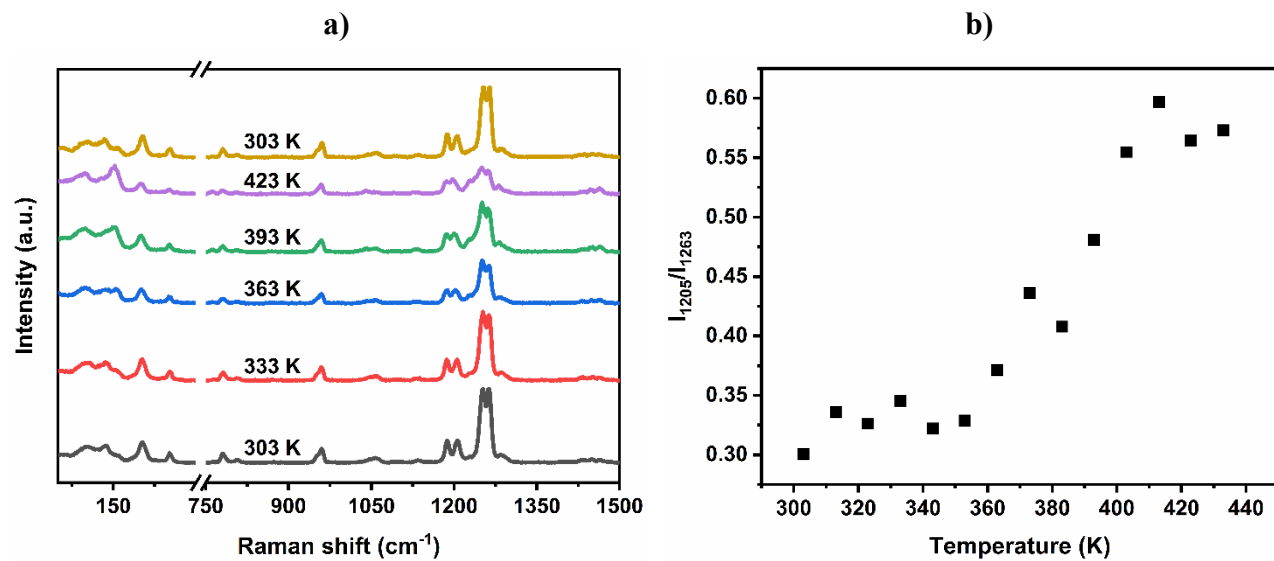


Figure S9. Raman spectra of **1** at different temperatures (**a**) and plot of 1205/1263 cm⁻¹ bands' integral intensity ratio as a function of temperature (**b**).

III- Mössbauer spectroscopy

Mössbauer spectra were recorded for **1·12H₂O**, intermediate phase obtained by heating of the hydrate at 328 K for 1 h and **1** at room temperature (Fig. S10). The spectra of the hydrate compound and the polymorphs display one doublet with hyperfine parameters indicating low spin state of Fe(II) in the examined samples: isomeric shift (δ^{LS}) values range from 0.632(3) mm s⁻¹ to 0.649(3) mm s⁻¹, while quadrupole splitting (ΔE_{Q}^{LS}) lies in 0.144(5)-0.207(6) mm s⁻¹ range.

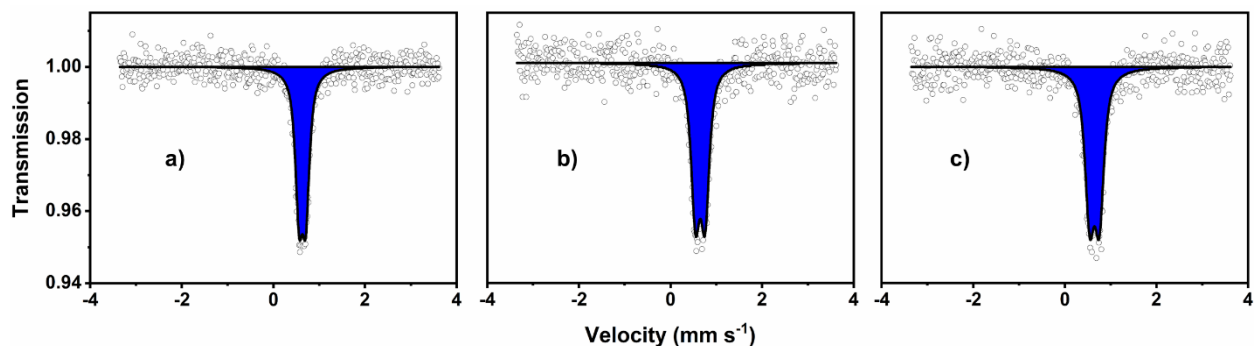


Figure S10. Room temperature Mössbauer spectra of crystalline **1·12H₂O** (a), intermediate phase (b) and powder of **1** (c).

IV- References

- 1 S. Rat, K. Ridier, L. Vendier, G. Molnár, L. Salmon and A. Bousseksou, *CrystEngComm*, 2017, **19**, 3271–3280.
- 2 J. D. Oliver, B. B. Hutchinson, D. F. Mullica and W. O. Milligan, *Inorg. Chem.*, 1980, **19**, 165–169.